Research article Open Access

Wanlin Wang, Guo Ping Wang*, Wang Zhang* and Di Zhang

Reversible thermochromic response based on photonic crystal structure in butterfly wing

DOI 10.1515/nanoph-2017-0025
Received February 13, 2017; revised April 19, 2017; accepted April 23, 2017

Abstract: Subtle responsive properties can be achieved by the photonic crystal (PC) nanostructures of butterfly based on thermal expansion effect. The studies focused on making the sample visually distinct. However, the response is restricted by limited thermal expansion coefficients. We herein report a new class of reversible thermochromic response achieved by controlling the ambient refractive index in butterfly PC structure. The photonic ethanol-filled nanoarchitecture sample is simply assembled by sealing liquid ethanol filling *Papilio ulysses* butterfly wing. Volatile ethanol is used to modulate the ambient refractive index. The sample is sealed with glasses to ensure reversibility. Liquid ethanol filling butterfly wing demonstrated significant allochroic response to ambient refractive index, which can be controlled by the liquefaction and vaporization of ethanol. This design is capable of converting thermal energy into visual color signals. The mechanism of this distinct response is simulated and proven by band theory. The response properties are performed with different filled chemicals and different structure parameters. Thus, the reversible thermochromic response design might have potential use in the fields such as detection, photonic switch, displays, and so forth.

***Corresponding authors: Guo Ping Wang,** College of Electronic Science and Technology and Guangdong Provincial Key Laboratory of Optoelectronic Micro/Nano Optomechatronics Engineering, Shenzhen University, Shenzhen 518060, China, e-mail: gpwang@szu.edu.cn; and **Wang Zhang,** State Key Laboratory of Metal Matrix Composites, Shanghai Jiao Tong University, Shanghai 200240, China, e-mail: wangzhang@sjtu.edu.cn
Wanlin Wang: College of Electronic Science and Technology and Guangdong Provincial Key Laboratory of Optoelectronic Micro/Nano Optomechatronics Engineering, Shenzhen University, Shenzhen 518060, China
Di Zhang: State Key Laboratory of Metal Matrix Composites, Shanghai Jiao Tong University, Shanghai 200240, China

Keywords: butterfly wing; photonic prystal; thermal response; thermochromic; finite-difference time-domain.

1 Introduction

The color of most creatures is relatively fixed, but some animals are capable of undergoing physiological color change, which allows them to show different colors in response to changing environment [1]. The color changes of animals can realize various functions, such as display, warning, camouflage, and communication. Thus, a series of color tunable photonic crystal (PC) materials was investigated with significant optical response under external stimuli [2–5]. These functions originated from well-defined physical properties such as high levels of sensitivity of reflectance/transmittance [6, 7]. The bioinspired materials based on butterfly wing PC structure have been proposed as next-generation materials, such as waveguides [8], dye-sensitized solar cells [9], gas response [10, 11], photo trappers [12], infrared detectors [13, 14], pH sensors [4], flat-panel displays [15], and photothermal materials [16, 17]. Nature is a perfect and great art gallery of new ideas and inspirations for designing and fabricating new PC structure, because the fittest surviving creatures evolved through brutal evolution and natural selection from one generation to another. The fine and subtle nanostructures of butterfly wing scales are the most well-known PC structure. These sophisticated structures have been designed as sensing materials [18–20]. They were designed and fabricated based on the relationship between the structures and their reflected lights.

Because of the structure's thermal expansion, the thermoresponsive sensors could be prepared, inspired by PC structure of butterfly wing. New infrared detectors were fabricated by doping butterfly scales with single-walled carbon nanotubes [13]. It was found that the reflectance spectra curve of the samples would be changed, when the ambient temperature was changed by infrared radiation. And better properties were achieved through depositing a layer of gold (Au) coating on butterfly wing [14]. Temperature responsivity of poly(N-isopropylacrylamide)-co-acrylic acid was also used to combine with the butterfly structure. The highest reflective peak exhibits 28-nm blue shift with an increase of 10°C in temperature. Unfortunately, it is difficult to make the sample more visually distinct with photonic-sensing materials. The optical response in these bio-inspired materials mainly resulted from thermal expansion [13, 14], while expansion was restricted by limited thermal expansion coefficients [21]. Thus, the requirement for new thermal sensors based on optical signal is sensitivity. The existing photonic-sensing material inspired by butterfly can only achieve a little wavelength response [22] or intensity response [13, 14] without changing color. New responsive mechanism is designed in this paper. A distinct color change and optical sensitivity were achieved by controlling the ambient refractive index in liquid ethanol filling photonic crystal (LEF-PC) using butterfly wing.

In this paper, we reported an experimental and simulated demonstration of a reversible thermochromic property based on LEF-PC with butterfly wing. Unlike many other bio-inspired studies using *Morpho* butterflies [18, 20, 22–24], *Papilio ulysses* butterfly wing was used in this paper because of the unique multilayer concavities [25–29], which show high color response with ambient refractive index [30, 31]. Here, *Papilio ulysses* butterfly wing with LEF-PC was sealed by double layers of glass. Liquefaction and vaporization of ethanol resulted from the external thermal stimulus were used to control the ambient refractive index. And then change on the ambient refractive index could be realized through visible response, which can be observed even by the naked eye. Ethanol acts as a bridge between thermal and biological PC structure, which further achieves the synergistic effect between thermal and optical response. Our experiments show that the periodic concave multilayer structure of *Papilio ulysses* butterfly wing exhibits visual distinct response to thermal stimulus. Color response was achieved by controlling the ambient refractive index result from liquefaction and vaporization of ethanol. Reversible response was shown by reflectance spectrum and digital photos. The following theoretical analysis validates that the change of ambient refractive index induces transformation of the sample, which brings about the optical response to external thermal stimulus. The key parameters *T* (the periodic concave multilayer structure) and RI (ambient refractive index) were theoretically simulated and discussed as optical response. Various color maps of response were achieved by simply designing parameters *T* and RI.

2 Methods

2.1 Reflectance measurements

Reflectance spectra of the sample were tested with a reflectance measurement setup based on a pair of optical fibers, one acting as the light source, the other acting as the light collector. A stabilized halogen light source was used for reflectance measurements.

2.2 Butterfly samples

Dried *Papilio ulysses* samples were chosen for this study. The bright blue across fore and hind dorsal wings scales were used to fabricate the sample.

2.3 Optical modeling

To theoretically analyze the optical response of the sample, we performed an optical response modeling inspired by the butterfly PC structure. The optical response was simulated by using the finite difference time domain (FDTD) method. In the optical model, we took into account the important contributor to the optical changes: a change in the refractive index induced by volatility. The scales of the butterflies are formed largely from chitin, whose refractive index was assumed to be $1.56+i0.06$ [32, 33]. In order to intensively study the parameters of the sample in a reasonable simulation time, we studied this problem by using two-dimensional (2D) periodic concave multilayer structure. The wavelength was defined to be between 400 and 800 nm. The proper mesh size was set to obtain a good trade-off between the computer memory requirement and the simulation time. And a convergence test was carefully performed.

2.4 From reflection to color

In order to reproduce the color response of the butterfly, we converted reflection into color map. Let us suppose that the butterfly is illuminated by an illuminant characterized by its energy distribution $D(\lambda)$. In this paper, we use the CIE (Commission Internationale de l'Eclairage) normalized illuminant D65, which closely matches that of the sky daylight [34]. Assuming that the butterfly has a reflectivity $R(\lambda)$, we can compute the CIE XYZ tristimulus values, which are one possible way to characterize the reflected color. We then transform the XYZ components into RGB components, which are more convenient for the imaging process. The last step is the color representation using MATLAB. We have replaced a complicated set of data [i.e. the spectrum R(λ)] by a color point in a color map. This representation can be very useful in obtaining the dynamic reflection properties. A 2D color map based on this representation has two free parameters (for example, the dynamic reflection of the butterfly with the process of volatilization).

3 Results and discussion

3.1 Sample characterization

Sparkling color and concave structure of the butterfly wing were shown in Figure 1. Unlike many other kinds of bio-inspired thermal responsive design using LEF-PC nanoarchitecture in *Morpho* butterfly [13, 14, 18, 22], *Papilio ulysses* butterfly scales were used as a LEF-PC nanoarchitecture in this paper. *Papilio ulysses* was used here because of its refractive index sensing property [30, 31]. The sparkling blue sections of *Papilio ulysses* were used in this study, as shown in Figure 1A. The uniform and dense scales were arranged on the surface of the wings regularly, as shown in Figure 1B. Scanning electron microscope (SEM) images shown in Figure 1C of the superficial layer of colored scales demonstrated that their surfaces to consist of a fairly regular array of concavities. Transmission electron microscope (TEM) images of the samples in cross-section highlighted the unique form of multilayer as shown in Figure 1D.

By a quite simple process, the LEF-PC nanoarchitecture sample was assembled with *Papilio ulysses* butterfly wing, as shown in Figure 2. Firstly, the butterfly wing was saturated with ethanol. Then the wing was sealed by two layers of glass and double-sided tape. The digital photo of the sample was shown in Figure 2B. Figure 2A and C shows the different optical microscopy images at 26°C and 32°C. And the corresponding 3D model was given in Figure 2E. Different parts of the sample were shown in Figure 2D. Part 2 is the butterfly wing saturated with reasonable quantity of ethanol. Then the butterfly was sealed with two sheet of glasses (part 1 and part 4) and

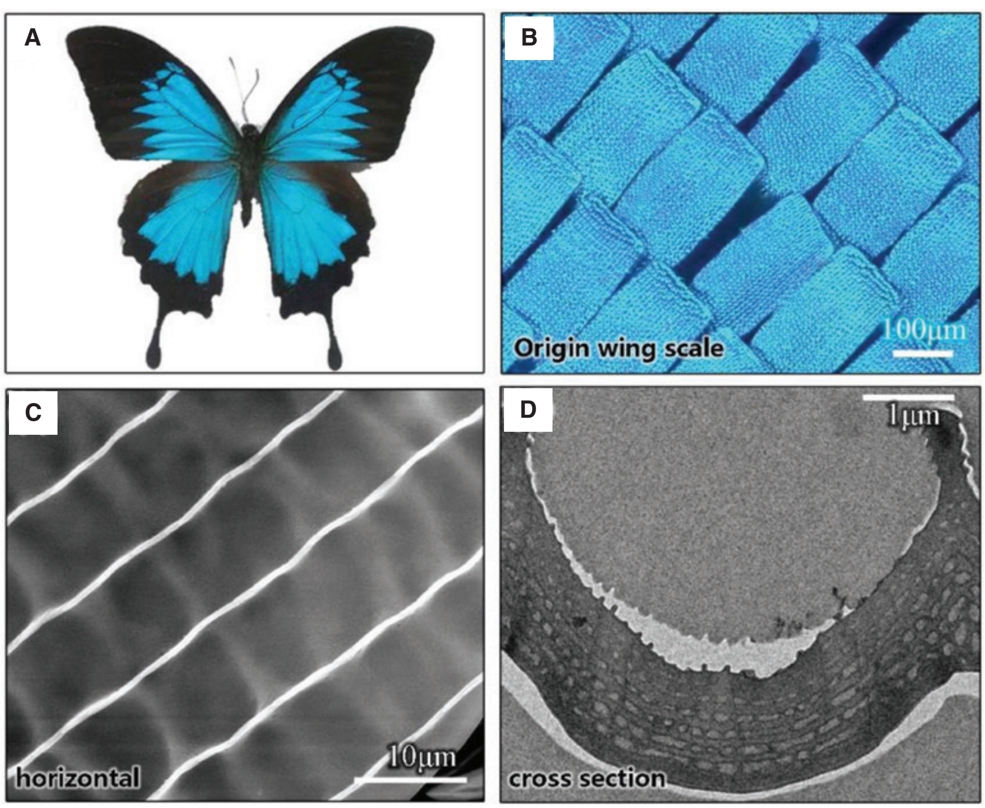

Figure 1: Sparkling color and periodic concave multilayer of the *Papilio ulysses* wing with PC structure. (A) Digital photo of natural *Papilio ulysses* butterfly. (B) Optical microscopy image of *Papilio ulysses* wing scale. (C) SEM micrograph of *Papilio ulysses* from a horizontal view. (D) TEM micrograph of *Papilio ulysses* from a cross-section view.

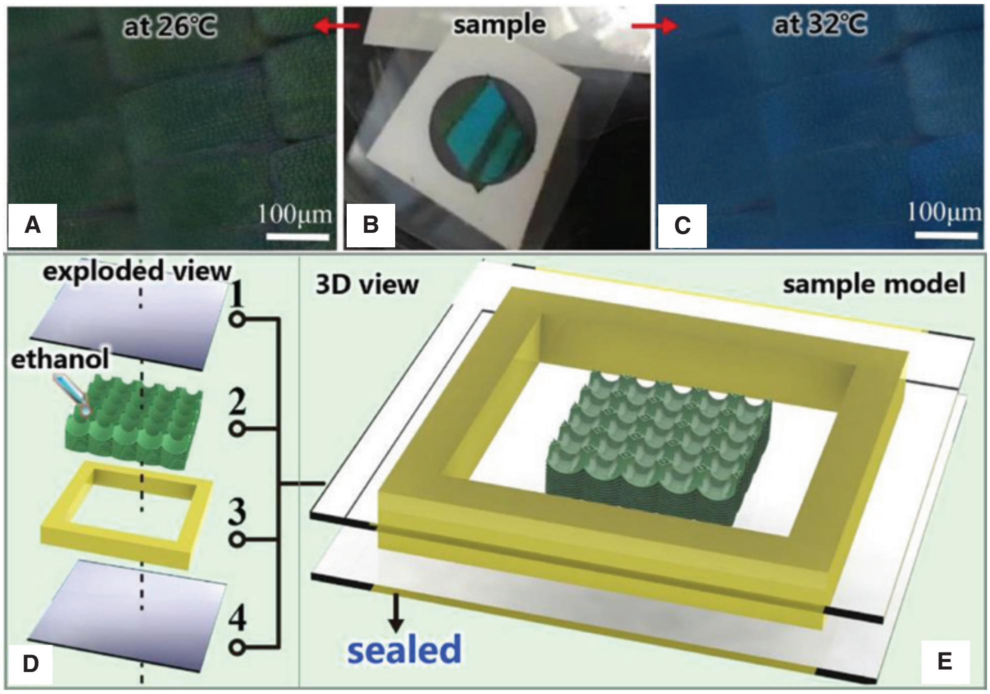

Figure 2: The LEF-PC sample fabricated by butterfly wing. (A, C) Optical microscopy images of the sample at 26°C and 32°C, respectively. (B) Digital photo of the sample, the wing was sealed by two layers of glass and double-sided tape. (D, E) Exploded view and 3D view models of the sample, part 1 and part 4 are glasses, part 2 is the butterfly wing saturated with ethanol, part 3 is the double-sided tape.

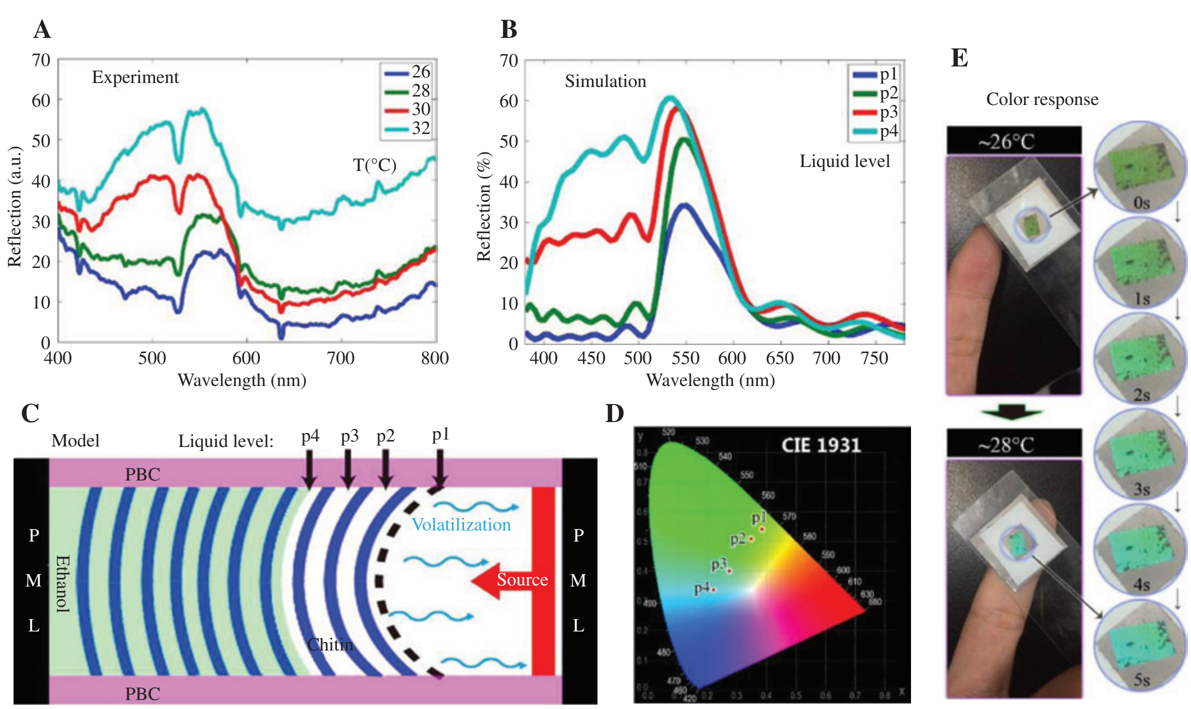

Figure 3: Thermochromic property of sealed PC wing sample with different temperatures. (A, B) Experiment and simulation reflectance under different temperatures (26°C, 28°C, 30°C and 32°C). (C) Structure model and boundary conditions. The boundary conditions in horizontal direction are absorbing (perfectly matched layer, PML) and in vertical direction are periodic (periodic boundary condition, PBC). A plane wave source illuminates the structure. Different liquid levels (p1, p2, p3, and p4) are used to characterize the increase of the temperature with the volatilization of the ethanol. (D) Color change calculated from corresponding reflectance in CIE chromaticity diagram with different temperatures. (E) Color response with different temperatures changed by contacting a finger, contact time is from 0 s to 5 s.

double-sided tape (part 3) to confirm the reversibility of the response.

3.2 Thermal-optical response

The thermochromic property of sealed butterfly wing sample was shown in Figure 3 under different temperatures. Experimental reflectance spectra under 26°C, 28°C, 30°C, and 32°C were measured and shown in Figure 3A. The peak of reflectance showed blue shift with the increase of temperature, as a new peak appeared in blue range, while the value of peak reflectance became higher with the increase of temperature. The width of reflectance spectra also increased significantly with higher temperature. All these effects control the thermochromic property of the sample. The response process was simulated to prove the conclusion of experimental results by FDTD method. The model for simulation is shown in Figure 3C. The boundary condition in horizontal directions is absorbing (perfectly matched layer, PML) and in vertical direction is periodic (periodic boundary condition, PBC). A plane wave source illuminates the structure. The increase in temperature can result in volatilization of the ethanol. Different liquid levels (p1, p2, p3, and p4) were used to characterize the increase of temperature. Simulated reflectance spectra of samples with different liquid levels were shown in Figure 3B. The simulation results agree well with the experimental conclusions. The peak wavelength blue shifts and the reflection value became higher with the increase of temperature. Here, we give simple explanation to this phenomenon. According to the theory of multilayer interference [35]: $m\lambda = 2(n_1 x_1 \cos\theta_1 + n_2 x_2 \cos\theta_2)$, the reflection peak is located at 560 nm in ethanol and located at 474 nm in air ($x_1 = 75$ nm and $x_2 = 120$ nm). Thus, with the increase of temperature, ethanol volatilizes, then the 474-nm peak becomes higher. The response of the wavelength and the peak value finally result in color response with different temperature. The color coordinate of the response was shown in Figure 3D by the CIE (Commission Internationale de l'Éclairage) (see Methods). The color response digital photos were displayed in Figure 3E with different temperature controlled by contacting a finger, and the contact time is from 0 s to 5 s. The whole process

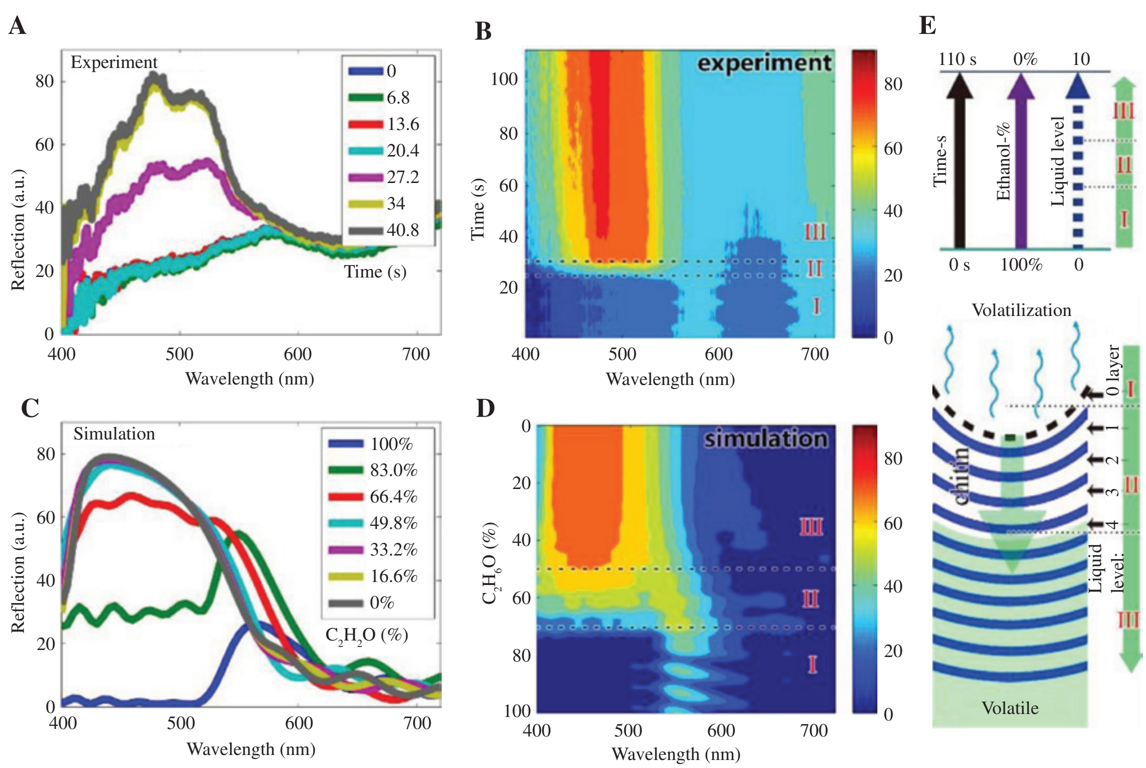

Figure 4: Experiment and simulation reflectance of butterfly wing (not sealed) with the natural vaporization of ethanol show the optical response process. (A, B) Line plot and contour plot of experiment reflectance considered as a function of time, the reflective data tested at 1.7-s intervals. (C, D) Line plot and contour plot of simulation reflectance considered as a function of different quantity of ethanol. (E) Diagram of the ethanol volatilization in periodic concave multilayer, the time of the volatilization is from 0 s to 110 s, the corresponding change of ethanol is from 100% to 0% (in simulation model), and the corresponding liquid level is changed from layer 0 to layer 10.

was shown in the video files in the supplementary data (video 1).

3.3 Reversible response

One of the most important properties of detection and sensor is response time. The response time of sealed PC butterfly wing with different temperatures was too short to be measured with time-resolved reflection spectra. Natural volatilization (without external thermal) of the original butterfly wing (not sealed) was applied here to achieve slower volatilization for studying the relationship between the volatilization processes in detail. Thus, the time-resolved reflection spectra can be measured. The experimental reflectance was considered as a function of time, as shown in Figure 4A and B. The diagram of ethanol volatilization was shown in Figure 4E. The reflectance spectra were tested at 1.7-s intervals to investigate the process of volatilization. It can be noted that the significant response of the wavelength and peak value are confirmed, as shown in Figure 4B, which is in agreement with the conclusion of sealed butterfly sample (Figure 3). The reflectance changed suddenly around 30 s. Thus, the optical response actually is a quick process. It means that the optical property is very sensitive with the volatilization of ethanol, which can change the ambient refractive index. It should be noticed that the response is not so big beside the sudden change. The corresponding line plot of the experimental data was shown in Figure 4A. The sudden change could be easily noted near 27.2 s. And the lines of the other time almost overlap before and after the sudden change. The response time of the color change is less than 5 s, and this result agrees well with the color change by contacting the finger, as shown in the supplementary data (video 1). It can be noted that reflectance spectra of the butterfly wing are noisy, as shown in Figure 3A and Figure 4A. The reason may be the small integration time of spectral testing. The time is small because the reflectance spectra were continuous and time-resolved. Although the reflectance spectra were noisy, the main reflectance peak of the butterfly in this paper was in agreement with the simulation and experiment results [25, 30].

In order to explain the experimental results, FDTD calculations were performed, as shown in Figure 4D. It

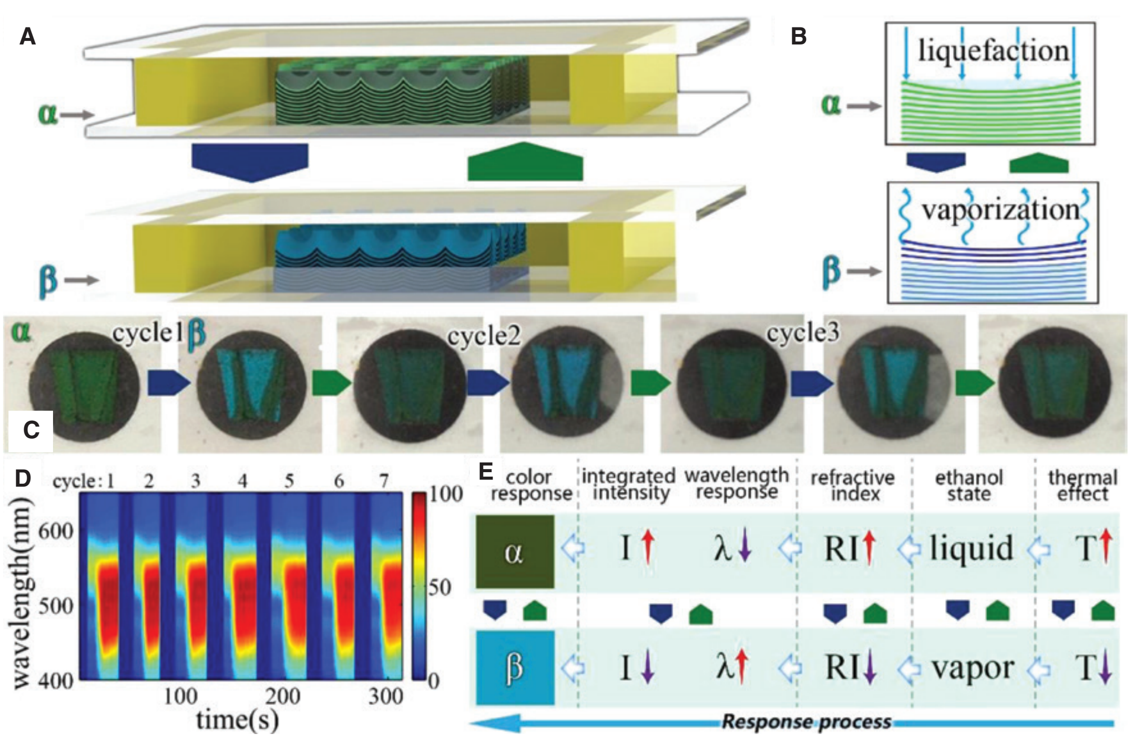

Figure 5: Reversibility of the thermochromic at multiple cyclings of the temperature. (A) The diagram of reversibility with α and β state (3D model), α: ethanol liquefaction, β: ethanol vaporization. (B) The diagram of reversibility with α and β states (2D model). (C) The digital photo of the sample at multiple cyclings of α and β states. (D) Dynamic response of LEF-PC sample in the visible spectral range. (E) Response process: thermal effect, ethanol state, refractive index, wavelength and intensity response, color response. The red and purple arrows mean the increase and decrease of the parameter.

is difficult to accurately label the quantity of the volatilization of ethanol in each interval with experimental method. Thus, the reflectance is considered as a function of percentage of ethanol rather than the function of time in simulation result, as shown in Figure 4E. The corresponding liquid level varies from 0 to 10 layers with the change of percent ethanol from 100% to 0% (in simulation model). The results are discussed in three parts, as shown in Figure 4E. Part I: The original liquid level was set about 580 nm above the structure. When ethanol in this part volatilized, the reflectance changed a little. And a similar phenomenon was confirmed by corresponding experiment data, as shown in Figure 4B. Part II: The liquid level from layer 0 to layer 4. In this part, the reflectance changed a lot, as shown in Figure 4B and D. The thickness of ethanol in this part is about 780 nm. Thus, the volatilization of this part achieved more significant response because of the change of ambient refractive index. Part III: The liquid level was from layer 5 to layer 10. In this part, the change in reflectance was little because most of the light reflected by the front layers. Thus, part II is the key part of the response mechanism in this design. Details about the response with layer 0 to layer 4 were studied in an analysis in the following paragraph.

Another important property to be considered for the sensing application is the reversibility of the sample. Reversibility of the reflectance was given in Figure 5 at multiple cycling of the temperature. The mechanism of the thermal response was shown in the diagram of reversibility with $T=26°C$ and $T=32°C$ (Figure 5A, B). The color of PC can be changed by modulation of ambient

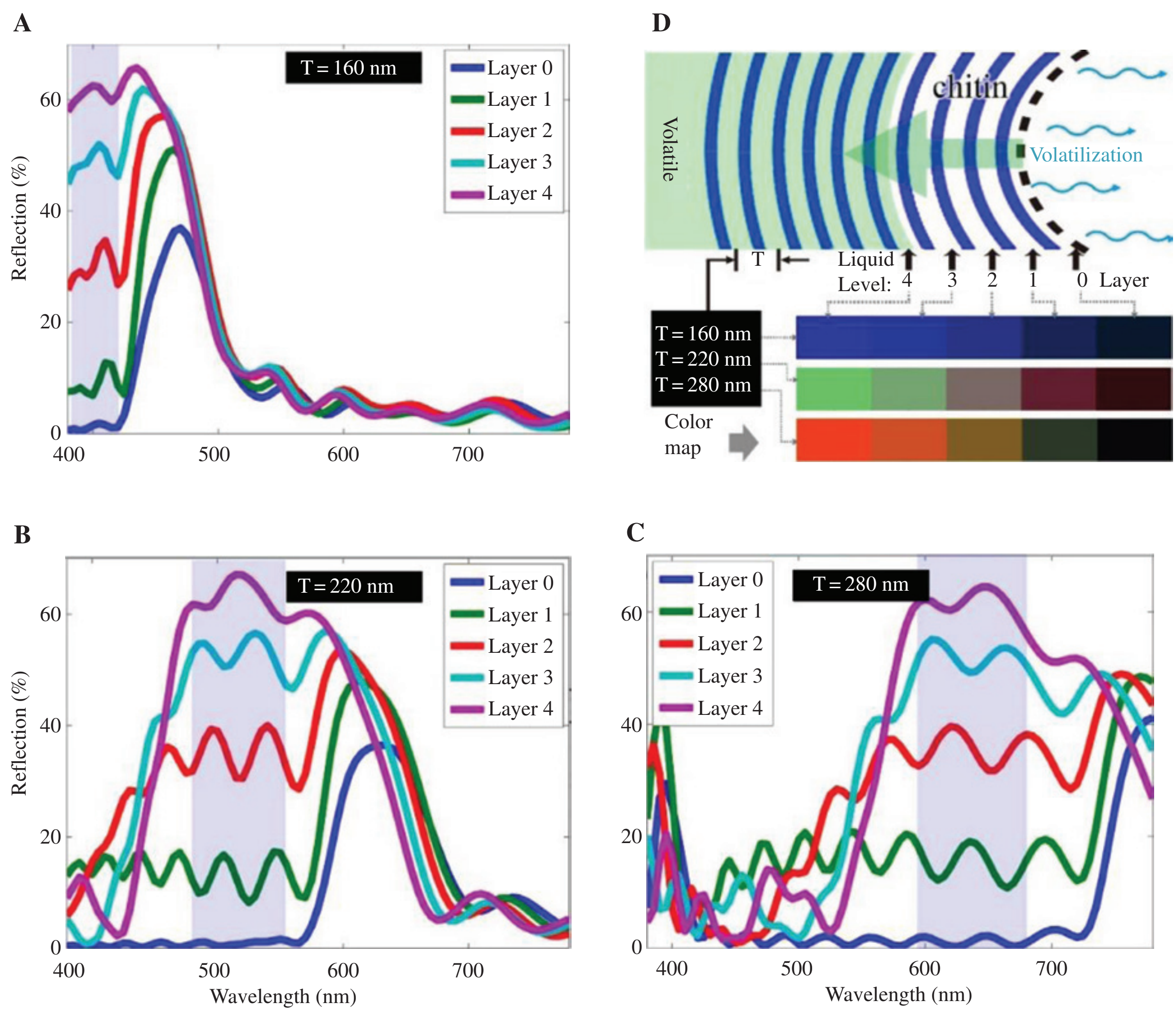

Figure 6: Computed reflectivity spectra show the effect of T (the period of periodic concave multilayer). (A, B, C) Reflectivity spectra with $T=160$ nm, 220 nm, and 280 nm, layers 0–4: the liquid level of ethanol, as shown in (D). (D) Schematic plot of the model shows the volatilization of ethanol, the liquid levels are labeled as 0 to 4. The color map with $T=160$ nm, 220 nm, and 280 nm was calculated from the corresponding reflectance.

refractive index. In this model, the ambient refractive index will be increased/decreased by the liquefaction/vaporization of the ethanol, as the liquefaction/vaporization of the ethanol is subjected to low/high temperature. The digital photo of the sample was shown in Figure 5C at multiple cyclings of $T=26°C$ and $T=32°C$. The whole process was shown in the video files in the supplementary data (video 2). The reversible thermochromic response can be observed. The real-time dynamic response of LEF-PC sample in the visible spectral range was given in Figure 5D. Here, seven cycles were presented. The reversed response conformed to the thermochromic property with this design. The result shows the high reversible response in wavelength and intensity. It can be seen that ethanol liquefaction and vaporization reversibly indicated a satisfactory durability of the LEF-PC sample. The reflectance of cooling period was not obtained because the light of the spectrophotometer was cut off. If the light was not cut off, the sample cannot be cooled down because of the heating effect of the light. As shown in Figure 5E, the process of the thermochromic property can be summarized as follows: thermal effect→ethanol state→refractive index→wavelength and intensity response→color response.

3.4 Structure parameters and different filled chemicals

The reversible thermochromic has been proven based on periodic concave multilayer in *Papilio ulysses* butterfly by using experimental and theoretical method. In the present case, the response properties were investigated with a fixed periodic concave multilayer model. Here, the

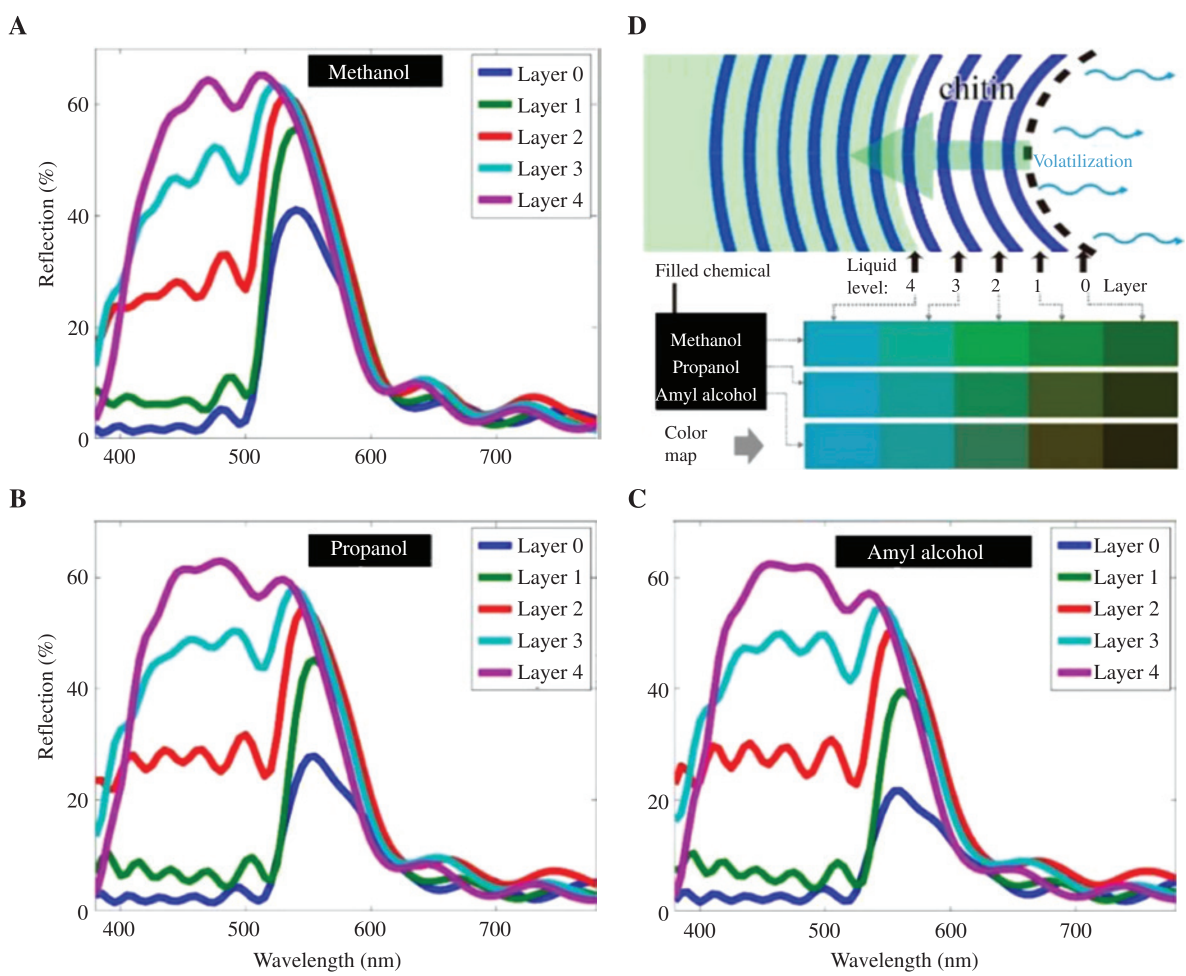

Figure 7: Computed reflectivity spectra show the effect of different filled chemicals: (A) methanol (refractive index = 1.33), (B) propanol (refractive index = 1.386), and (C) amyl alcohol (refractive index = 1.411). Layers 0–4: the liquid level of ethanol shown in (D). (D) Schematic plot of the model shows the volatilization of the ethanol, the liquid levels are labeled as 0 to 4. The color map with different filled chemicals was calculated from the corresponding reflectance.

color response properties are discussed with the periodic concave multilayer characterized by *T* (the period of periodic concave multilayer) and different filled chemicals (ambient refractive index). The effect of *T* was shown in Figure 6. Figure 6D shows the schematic plot of the model with the volatilization of ethanol. Liquid levels 0 to 4 were simulated according to the results in Figure 4. The effect of parameter *T* to the optical response can be summarized as follows: (1) The optical response to reflectance peak intensity changed a little with different *T* values. (2) The optical responses to reflectance peak wavelength increased with higher *T* values. All these effects control the appearance of color response of the sample, as shown at the bottom of Figure 6D. Different response color map can be achieved by simply changing parameter *T*.

As shown in Figure 7, optical response properties were obtained with different filled chemicals: (a) methanol (refractive index = 1.33), (b) propanol (refractive index = 1.386), and (c) amyl alcohol (refractive index = 1.411). The effect of the parameter refractive index to the optical response can be summarized as follows:

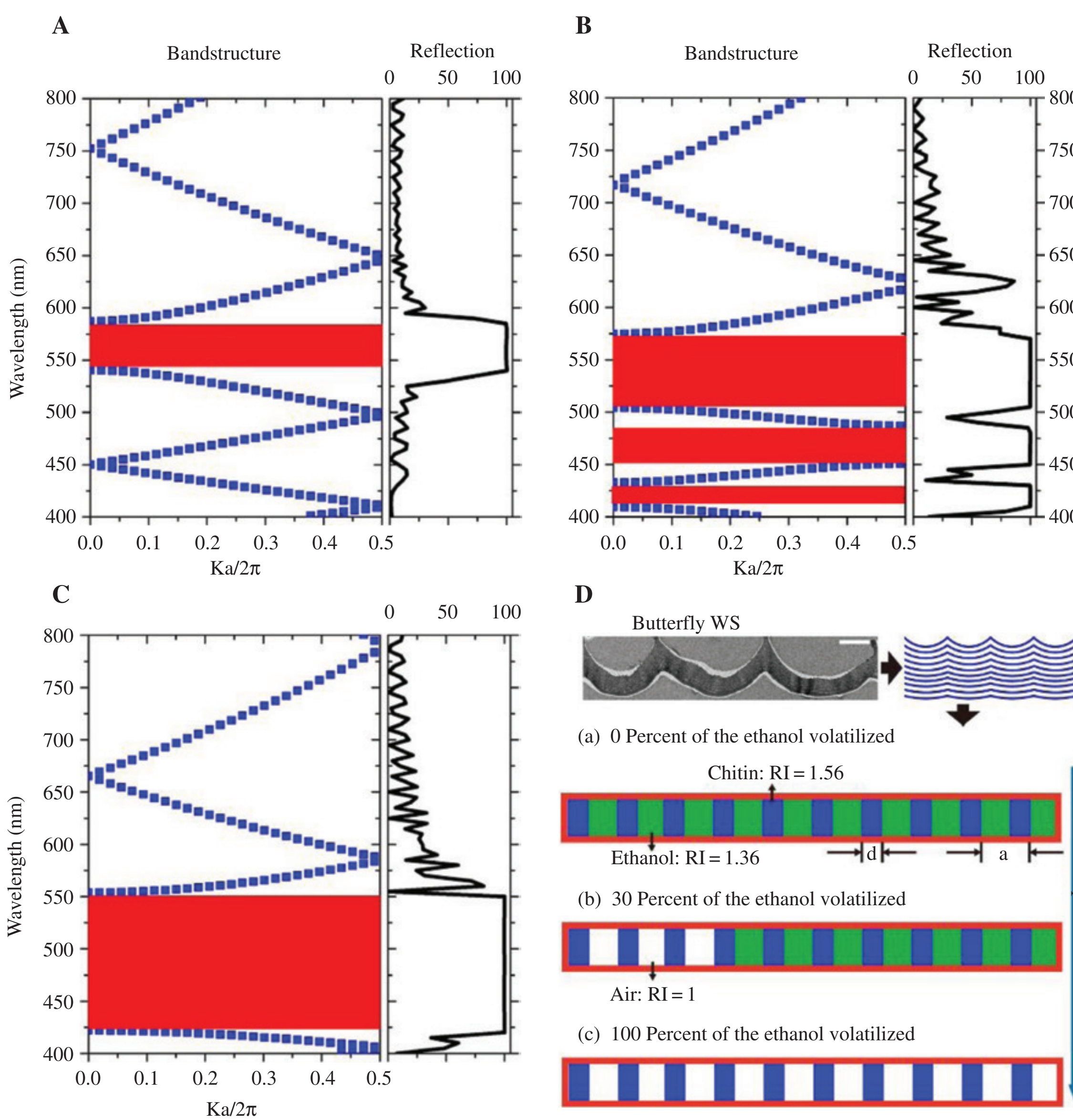

Figure 8: Band diagram and corresponding reflection with volatilization of the ethanol in *Papilio ulysses* PC structure, simplified 1D model was applied here. (A) Zero percent of the ethanol volatilized. (B) Thirty percent of the ethanol volatilized. (C) One hundred percent of the ethanol volatilized. (D) Schematic plot of the PC model used in (a, b, c). Zero percent, 30%, and 100% of the ethanol volatilized, respectively. The refractive index of the chitin: 1.56; the refractive index of ethanol: 1.36; the refractive index of the air: 1.

(1) The optical response increased with higher refractive index values. (2) The optical responses mainly result from the change of reflectance peak intensity rather than reflectance peak wavelength. All these effects control the appearance of color response of the sample, as shown at the bottom of Figure 7D. Thus, different color maps can be achieved by simply designing the parameters *T* and refractive index.

3.5 Photonic bandgap analysis

The mechanism of this optical response can be investigated by the theory of PC. Band diagram and corresponding reflection were shown in Figure 8 with volatilization of the ethanol in *Papilio ulysses* PC structure. The simplified 1D model was applied here. Zero percent, 30%, and 100% of ethanol volatilized in Figure 8A, B, and C, respectively. The models were shown in Figure 8D. The width of reflectance increased significantly with higher temperature, which was observed in Figures 3 and 4. Thus, the band width increased with volatilization of ethanol. This conclusion can be confirmed by the band diagram in Figure 8A, B, and C.

4 Conclusions

In summary, the reversible thermochromic property of LEF-PC inspired by *Papilio ulysses* was investigated both by experiment and theoretical simulation. In this paper, the ambient refractive index was chosen as the bridge between thermal and biological PC structure to replace the thermal expansion because of the limited thermal expansion coefficients. Volatile ethanol was used in the sample to modulate the ambient refractive index, while the sample was sealed with glasses to ensure reversibility. LEF-PC presents significant effect between reflectance and ambient refractive index, which can be controlled by the liquefaction and vaporization of ethanol. The design is capable of converting thermal energy into visually optical signals. The results show visually distinct reversible response in wavelength and intensity. High sensitivity can be achieved and the color response can be observed even by the naked eye. This study is only the first step in the discovery and design of new ideal stimuli-responsive materials of hierarchical photonic structures. The new design holds great potential use in fields such as detection, sensor, photonic switch, displays, and so forth.

Acknowledgments: This work was supported by the National Natural Science Foundation of China (Grant Nos. 51602205, 11274247, 51572169, 11574218, 11504243, and 11604217), Natural Science Foundation of Guangdong Province, China (Grant no. 2016A030313042, 2015A030310400), Shanghai Rising-Star Program (16QA1402400), the Science and Technology Innovation Commission of Shenzhen (Grant No. JCYJ20160520165724531), and the Fundamental Research Funds for the Shenzhen University (Grant No. 2016025).

References

[1] Ligon RA, McGraw KJ. Chameleons communicate with complex colour changes during contests: different body regions convey different information. Biol Lett 2013;9: 20130892.
[2] Sorrell CD, Carter MCD, Serpe MJ. Color tunable poly (N-Isopropylacrylamide)-co-acrylic acid microgel–Au hybrid assemblies. Adv Funct Mater 2011;21:425–33.
[3] Xu X, Friedman G, Humfeld KD, Majetich SA, Asher SA. Superparamagnetic photonic crystals. Adv Mater 2001;13:1681.
[4] Yang Q, Zhu S, Peng W, et al. Bioinspired fabrication of hierarchically structured, pH-tunable photonic crystals with unique transition. ACS Nano 2013;7:4911–18.
[5] Lee YJ, Braun PV. Tunable inverse opal hydrogel pH sensors. Adv Mater 2003;15:563–6.
[6] Plößer K. Optical properties of photonic crystals, K. Sakoda. Springer, Berlin, 2001. ISBN: 3-540-41199-2.
[7] Nair RV, Vijaya R. Photonic crystal sensors: an overview. Prog Quant Electron 2010;34:89–134.
[8] Huang JY, Wang XD, Wang ZL. Controlled replication of butterfly wings for achieving tunable photonic properties. Nano Lett 2006;6:2325–31.
[9] Zhang W, Zhang D, Fan T, et al. Novel photoanode structure templated from butterfly wing scales. Chem Mater 2009;21: 33–40.
[10] Mouchet SR, Tabarrant T, Lucas S, Su B-L, Vukusic P, Deparis O. Vapor sensing with a natural photonic cell. Opt Express 2016;24:12267–80.
[11] Potyrailo RA, Ghiradella H, Vertiatchikh A, Dovidenko K, Cournoyer JR, Olson E. Morpho butterfly wing scales demonstrate highly selective vapour response. Nat Photonics 2007;1:123–8.
[12] Han Z, Shang C, Liu Z, Ren L. Light trapping structures in wing scales of butterfly Trogonoptera Brookiana. Nanoscale 2012;4:2879–83.
[13] Pris AD, Utturkar Y, Surman C, et al. Towards high-speed imaging of infrared photons with bio-inspired nanoarchitectures. Nat Photonics 2012;6:195–200.
[14] Zhang F, Shen Q, Shi X, et al. Infrared detection based on localized modification of Morpho butterfly wings. Adv Mater 2014;27:1077–82.
[15] Kustandi TS, Low HY, Teng JH, Rodriguez I, Yin R. Mimicking domino-like photonic nanostructures on butterfly wings. Small 2009;5:574–8.

[16] Tian J, Zhang W, Gu J, Deng T, Zhang D. Bioinspired Au–CuS coupled photothermal materials: enhanced infrared absorption and photothermal conversion from butterfly wings. Nano Energy 2015;17:52–62.
[17] Wu L, Ren W, Song Y, Xin M, Niu S, Han Z. High light absorption properties and optical structures in butterfly Heliophorus ila Lvcaenidae wing scales. RSC Adv 2015;5:46011–6.
[18] Li Q, Zeng Q, Shi L, Zhang X, Zhang K-Q. Bio-inspired sensors based on photonic structures of Morpho butterfly wings: a review. J Mater Chem C 2016;4:1752–63.
[19] Zhang J, Liang Y, Mao J, et al. 3D microporous Co_3O_4-carbon hybrids biotemplated from butterfly wings as high performance VOCs gas sensor. Sens Actuators B Chem 2016;235:420–31.
[20] Niu S, Li B, Mu Z, et al. Excellent structure-based multifunction of Morpho butterfly wings: a review. J Bionic Eng 2015;12:170–89.
[21] Wada M, Saito Y. Lateral thermal expansion of chitin crystals. J Polym Sci Part B Polym Phys 2001;39:168–74.
[22] Xu D, Yu H, Xu Q, Xu G, Wang K. Thermoresponsive photonic crystal: synergistic effect of poly (N-isopropylacrylamide)-co-acrylic acid and Morpho butterfly wing. ACS Appl Mater Interfaces 2015;7:8750–6.
[23] Shen Q, He J, Ni M, et al. Subtractive structural modification of Morpho butterfly wings. Small 2015;11:5705–11.
[24] Potyrailo RA, Bonam RK, Hartley JG, et al. Towards outperforming conventional sensor arrays with fabricated individual photonic vapour sensors inspired by Morpho butterflies. Nat Commun 2015;6:7959.
[25] Vukusic P, Sambles R, Lawrence C, Wakely G. Sculpted-multilayer optical effects in two species of Papilio butterfly. Appl Opt 2001;40:1116–25.
[26] Lo M-L, Li W-H, Tseng S-Z, Chen S-H, Chan C-H, Lee C-C. Replica of the structural color for Papilio blumei butterfly. J Nanophotonics 2013;7:073597.
[27] Diao YY, Liu XY. Mysterious coloring: structural origin of color mixing for two breeds of Papilio butterflies. Opt Express 2011;19:9232–41.
[28] Liu F, Wang GB, Jiang LP, Dong BQ. Structural colouration and optical effects in the wings of Papilio peranthus. J Opt-Uk 2010;12:065301.
[29] Kolle M, Salgard-Cunha PM, Scherer MRJ, et al. Mimicking the colourful wing scale structure of the Papilio blumei butterfly. Nat Nanotechnol 2010;5:511–5.
[30] Wang W, Zhang W, Fang X, et al. Demonstration of higher colour response with ambient refractive index in Papilio blumei as compared to Morpho rhetenor. Sci Reports 2014;4:5591.
[31] Isnaeni, Muslimin AN, Birowosuto MD. AIP Conference Proceedings 2016;1:030001.
[32] Vukusic P, Sambles JR, Lawrence CR, Wootton RJ. Quantified interference and diffraction in single Morpho butterfly scales. Proc R Soc Lond B 1999;266:1403–11.
[33] Stavenga DG, Leertouwer HL, Wilts BD. Quantifying the refractive index dispersion of a pigmented biological tissue using Jamin-Lebedeff interference microscopy. Light Sci Appl 2013;2:e100.
[34] Stockman A. Colour & Vision Research laboratory and database, http://www.cvrl.org/.
[35] Kinoshita S, Yoshioka S, Miyazaki J. Physics of structural colors. Rep Prog Phys 2008;71:076401.

Supplemental Material: The online version of this article (DOI: 10.1515/nanoph-2017-0025) offers supplementary material, available to authorized users.